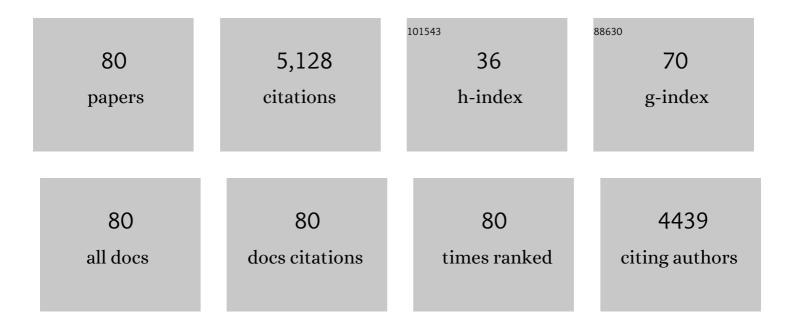
## Mark D Schmitz

List of Publications by Year in descending order

Source: https://exaly.com/author-pdf/8563995/publications.pdf Version: 2024-02-01



MADE D SCHMITZ

#	Article	IF	CITATIONS
1	Calibrating the Cryogenian. Science, 2010, 327, 1241-1243.	12.6	488
2	Reassessing the uranium decay constants for geochronology using ID-TIMS U–Pb data. Geochimica Et Cosmochimica Acta, 2006, 70, 426-445.	3.9	406
3	Derivation of isotope ratios, errors, and error correlations for Uâ€Pb geochronology using <sup>205</sup> Pbâ€ <sup>235</sup> Uâ€( <sup>233</sup> U)â€spiked isotope dilution thermal ionization mass spectrometric data. Geochemistry, Geophysics, Geosystems, 2007, 8, .	2.5	320
4	U-Pb zircon and titanite systematics of the Fish Canyon Tuff: an assessment of high-precision U-Pb geochronology and its application to young volcanic rocks. Geochimica Et Cosmochimica Acta, 2001, 65, 2571-2587.	3.9	297
5	Ages and origins of rocks of the Killingworth dome, south-central Connecticut: Implications for the tectonic evolution of southern New England. Numerische Mathematik, 2007, 307, 63-118.	1.4	185
6	Palaeontological evidence for an Oligocene divergence between Old World monkeys and apes. Nature, 2013, 497, 611-614.	27.8	180
7	Subduction and terrane collision stabilize the western Kaapvaal craton tectosphere 2.9 billion years ago. Earth and Planetary Science Letters, 2004, 222, 363-376.	4.4	172
8	MKED1: A new titanite standard for in situ analysis of Sm–Nd isotopes and U–Pb geochronology. Chemical Geology, 2016, 425, 110-126.	3.3	153
9	Forearc ages reveal extensive short-lived and rapid seafloor spreading following subduction initiation. Earth and Planetary Science Letters, 2019, 506, 520-529.	4.4	148
10	Evaluation of Duluth Complex anorthositic series (AS3) zircon as a U-Pb geochronological standard: new high-precision isotope dilution thermal ionization mass spectrometry results. Geochimica Et Cosmochimica Acta, 2003, 67, 3665-3672.	3.9	130
11	Magma emplacement, differentiation and cooling in the middle crust: Integrated zircon geochronological–geochemical constraints from the Bergell Intrusion, Central Alps. Chemical Geology, 2015, 417, 322-340.	3.3	125
12	Neoarchean paleoweathering of tonalite and metabasalt: Implications for reconstructions of 2.69Ga early terrestrial ecosystems and paleoatmospheric chemistry. Precambrian Research, 2011, 189, 1-17.	2.7	121
13	Mesozoic thermal evolution of the southern African mantle lithosphere. Lithos, 2003, 71, 273-287.	1.4	118
14	Constraints on the thermal evolution of continental lithosphere from U-Pb accessory mineral thermochronometry of lower crustal xenoliths, southern Africa. Contributions To Mineralogy and Petrology, 2003, 144, 592-618.	3.1	98
15	Chronostratigraphy and Paleoclimatology of the LodÃ <sup>∵</sup> ve Basin, France: Evidence for a pan-tropical aridification event across the Carboniferous–Permian boundary. Palaeogeography, Palaeoclimatology, Palaeoecology, 2015, 430, 118-131.	2.3	98
16	Sm–Nd isotope systematics by laser ablation-multicollector-inductively coupled plasma mass spectrometry: Methods and potential natural and synthetic reference materials. Chemical Geology, 2011, 284, 1-20.	3.3	96
17	Age intercalibration of 40Ar/39Ar sanidine and chemically distinct U/Pb zircon populations from the Alder Creek Rhyolite Quaternary geochronology standard. Chemical Geology, 2013, 345, 87-98.	3.3	96
18	Ultrahigh-temperature metamorphism in the lower crust during Neoarchean Ventersdorp rifting and magmatism, Kaapvaal Craton, southern Africa. Bulletin of the Geological Society of America, 2003, 115, 533-548.	3.3	91

MARK D SCHMITZ

#	Article	IF	CITATIONS
19	Decoupling of the Lu-Hf and Sm-Nd isotope systems during the evolution of granulitic lower crust beneath southern Africa. Geology, 2004, 32, 405.	4.4	83
20	A review of the Middle–Late Pennsylvanian west European regional substages and floral biozones, and their correlation to the Geological Time Scale based on new U–Pb ages. Earth-Science Reviews, 2016, 154, 301-335.	9.1	81
21	High-precision U–Pb zircon age constraints on the Carboniferous–Permian boundary in the southern Urals stratotype. Earth and Planetary Science Letters, 2007, 256, 244-257.	4.4	72
22	Understanding cratonic flood basalts. Earth and Planetary Science Letters, 2006, 245, 190-201.	4.4	69
23	Rapid magma evolution constrained by zircon petrochronology and 40Ar/39Ar sanidine ages for the Huckleberry Ridge Tuff, Yellowstone, USA. Geology, 2014, 42, 643-646.	4.4	68
24	Cryogenian of Yukon. Precambrian Research, 2018, 319, 114-143.	2.7	68
25	EOCENE ZIRCON REFERENCE MATERIAL FOR MICROANALYSIS OF U-Th-Pb ISOTOPES AND TRACE ELEMENTS. Canadian Mineralogist, 2014, 52, 409-421.	1.0	65
26	Exploring the law of detrital zircon: LA-ICP-MS and CA-TIMS geochronology of Jurassic forearc strata, Cook Inlet, Alaska, USA. Geology, 2019, 47, 1044-1048.	4.4	63
27	South Australian U-Pb zircon (CA-ID-TIMS) age supports globally synchronous Sturtian deglaciation. Precambrian Research, 2018, 315, 257-263.	2.7	58
28	Filling the gap: new precise Early Cretaceous radioisotopic ages from the Andes. Geological Magazine, 2015, 152, 557-564.	1.5	56
29	The Petrology of the Rotoiti Eruption Sequence, Taupo Volcanic Zone: an Example of Fractionation and Mixing in a Rhyolitic System. Journal of Petrology, 2004, 45, 2045-2066.	2.8	55
30	The significance of U–Pb zircon dates in lower crustal xenoliths from the southwestern margin of the Kaapvaal craton, southern Africa. Chemical Geology, 2001, 172, 59-76.	3.3	53
31	Kikiktat volcanics of Arctic Alaska—Melting of harzburgitic mantle associated with the Franklin large igneous province. Lithosphere, 2015, 7, 275-295.	1.4	50
32	Cambrian Sauk transgression in the Grand Canyon region redefined by detrital zircons. Nature Geoscience, 2018, 11, 438-443.	12.9	50
33	High-precision U-Pb zircon ages for explosive volcanism calibrating the NW European continental Autunian stratotype. Gondwana Research, 2017, 51, 118-136.	6.0	45
34	A high precision U–Pb radioisotopic age for the Agrio Formation, Neuquén Basin, Argentina: Implications for the chronology of the Hauterivian Stage. Cretaceous Research, 2017, 75, 193-204.	1.4	44
35	Pre- to synglacial rift-related volcanism in the Neoproterozoic (Cryogenian) Pocatello Formation, SE Idaho: New SHRIMP and CA-ID-TIMS constraints. Lithosphere, 2013, 5, 128-150.	1.4	41
36	Westward Growth of Laurentia by Pre–Late Jurassic Terrane Accretion, Eastern Oregon and Western Idaho, United States. Journal of Geology, 2015, 123, 233-267.	1.4	40

MARK D SCHMITZ

#	Article	IF	CITATIONS
37	Interhemispheric radio-astrochronological calibration of the time scales from the Andean and the Tethyan areas in the Valanginian–Hauterivian (Early Cretaceous). Gondwana Research, 2019, 70, 104-132.	6.0	39
38	An improved approach to age-modeling in deep time: Implications for the Santa Cruz Formation, Argentina. Bulletin of the Geological Society of America, 2020, 132, 233-244.	3.3	36
39	Astronomical forcing of Carboniferous paralic sedimentary cycles in the Upper Silesian Basin, Czech Republic (Serpukhovian, latest Mississippian): New radiometric ages afford an astronomical age model for European biozonations and substages. Earth-Science Reviews, 2018, 177, 715-741.	9.1	33
40	New insights on the Orosirian carbon cycle, early Cyanobacteria, and the assembly of Laurentia from the Paleoproterozoic Belcher Group. Earth and Planetary Science Letters, 2019, 520, 141-152.	4.4	31
41	High-precision U–Pb zircon age constraints on the duration of rapid biogeochemical events during the Ludlow Epoch (Silurian Period). Journal of the Geological Society, 2015, 172, 157-160.	2.1	30
42	Coupled Re-Os and U-Pb geochronology of the Tonian Chuar Group, Grand Canyon. Bulletin of the Geological Society of America, 2018, 130, 1085-1098.	3.3	30
43	A middle–late Ediacaran volcanoâ€sedimentary record from the eastern Arabianâ€Nubian shield. Terra Nova, 2014, 26, 120-129.	2.1	29
44	An ultrasonic method for isolating nonclay components from clayâ€rich material. Geochemistry, Geophysics, Geosystems, 2014, 15, 492-498.	2.5	29
45	Geochronological constraints on Neoproterozoic rifting and onset of the Marinoan glaciation from the Kingston Peak Formation in Death Valley, California (USA). Geology, 2020, 48, 1083-1087.	4.4	29
46	One diamictite and two rifts: Stratigraphy and geochronology of the Gataga Mountain of northern British Columbia. Numerische Mathematik, 2018, 318, 167-207.	1.4	28
47	Terrestrial and marginal-marine record of the mid-Cretaceous Oceanic Anoxic Event 2 (OAE 2): High-resolution framework, carbon isotopes, CO2 and sea-level change. Palaeogeography, Palaeoclimatology, Palaeoecology, 2019, 524, 118-136.	2.3	27
48	U–Pb and Hf isotopic analysis of zircon in lower crustal xenoliths from the Navajo volcanic field: 1.4ÂGa mafic magmatism and metamorphism beneath the Colorado Plateau. Contributions To Mineralogy and Petrology, 2006, 151, 313-330.	3.1	25
49	Settling the issue of "decoupling―between atmospheric carbon dioxide and global temperature: [CO2]atm reconstructions across the warming Paleogene-Neogene divide. Geology, 2017, 45, 999-1002.	4.4	25
50	New toxodontid (Notoungulata) from the Early Miocene of Mendoza, Argentina. Palaontologische Zeitschrift, 2015, 89, 611-634.	1.6	24
51	Rapid emplacement of massive Duluth Complex intrusions within the North American Midcontinent Rift. Geology, 2021, 49, 185-189.	4.4	21
52	Apatites for destruction: Reference apatites from Morocco and Brazil for U-Pb petrochronology and Nd and Sr isotope geochemistry. Chemical Geology, 2022, 590, 120689.	3.3	21
53	A detrital zircon test of large-scale terrane displacement along the Arctic margin of North America. Geology, 2021, 49, 545-550.	4.4	20
54	Chronostratigraphic Revision of the Cloverly Formation (Lower Cretaceous, Western Interior, USA). Bulletin of the Peabody Museum of Natural History, 2019, 60, 3.	1.1	17

MARK D SCHMITZ

#	Article	IF	CITATIONS
55	The Main Ostrava Whetstone: composition, sedimentary processes, palaeogeography and geochronology of a major Mississippian volcaniclastic unit of the Upper Silesian Basin (Poland and) Tj ETQq1	10.78448314 r	gBId∕Overlo
56	Middle Triassic lake deepening in the Ordos Basin of North China linked with global sea-level rise. Global and Planetary Change, 2021, 207, 103670.	3.5	15
57	Volcanic Initiation of the Eocene Heart Mountain Slide, Wyoming, USA. Journal of Geology, 2017, 125, 439-457.	1.4	14
58	Strain variations across the Proterozoic Penokean Orogen, USA and Canada. Precambrian Research, 2018, 318, 25-69.	2.7	14
59	Precise early Cambrian U–Pb zircon dates bracket the oldest trilobites and archaeocyaths in Moroccan West Gondwana. Geological Magazine, 2021, 158, 219-238.	1.5	14
60	Integrating zircon trace-element geochemistry and high-precision U-Pb zircon geochronology to resolve the timing and petrogenesis of the late Ediacaran–Cambrian Wichita igneous province, Southern Oklahoma Aulacogen, USA. Geology, 2021, 49, 268-272.	4.4	14
61	Climate- and eustasy-driven cyclicity in Pennsylvanian fusulinid assemblages, Donets Basin (Ukraine). Palaeogeography, Palaeoclimatology, Palaeoecology, 2014, 396, 41-61.	2.3	13
62	Isotopic evidence for a lithospheric origin of alkaline rocks and carbonatites: an example from southern Africa. Canadian Journal of Earth Sciences, 2016, 53, 1216-1226.	1.3	13
63	A link between rift-related volcanism and end-Ediacaran extinction? Integrated chemostratigraphy, biostratigraphy, and U-Pb geochronology from Sonora, Mexico. Geology, 2021, 49, 115-119.	4.4	13
64	(Re)proposal of three Cambrian Subsystems and their Geochronology. Episodes, 2021, 44, 273-283.	1.2	13
65	Coal-bearing fluvial cycles of the late Paleozoic tropics; astronomical control on sediment supply constrained by high-precision radioisotopic ages, Upper Silesian Basin. Earth-Science Reviews, 2022, 228, 103998.	9.1	13
66	Comparing desired workforce skills and reported teaching practices to model students' experiences in undergraduate geoscience programs. Journal of Geoscience Education, 2021, 69, 27-42.	1.4	11
67	TS-Mnz – A new monazite age reference material for U-Th-Pb microanalysis. Chemical Geology, 2021, 572, 120195.	3.3	11
68	New high-precision U-Pb zircon age of the Irati Formation (ParanÃ <sub>i</sub> Basin) and implications for the timing of the Kungurian anoxic events recorded in southern Gondwana. Gondwana Research, 2022, 107, 134-145.	6.0	11
69	The duration of a Yellowstone super-eruption cycle and implications for the age of the Olduvai subchron. Earth and Planetary Science Letters, 2017, 479, 377-386.	4.4	9
70	Volcanism at 1.45†Ma within the Yellowstone Volcanic Field, United States. Journal of Volcanology and Geothermal Research, 2018, 357, 224-238.	2.1	9
71	A new late Hemingfordian vertebrate fauna from Hawk Rim, Oregon, with implications for biostratigraphy and geochronology. Journal of Vertebrate Paleontology, 2016, 36, e1201095.	1.0	7
72	Depositional settings and changing composition of the Jambi palaeoflora within the Permian Mengkarang Formation (Sumatra, Indonesia). Geological Journal, 2018, 53, 2969-2990.	1.3	7

#	Article	IF	CITATIONS
73	A new, high-precision CA-ID-TIMS date for the â€~Kalkberg' K-bentonite (Judds Falls Bentonite). Lethaia, 2018, 51, 344-356.	1.4	7
74	A robust age model for the Cryogenian Pocatello Formation of southeastern Idaho (northwestern) Tj ETQqO O O zircons. , 2022, 18, 825-849.	rgBT /Over	lock 10 Tf 50 6
75	The radioisotopically constrained Viséan onset of turbidites in the Moravian-Silesian part of the Rhenohercynian foreland basin (Central European Variscides). International Journal of Earth Sciences, 2018, 107, 711-727.	1.8	5
76	Timescales of impact melt sheet crystallization and the precise age of the Morokweng impact structure, South Africa. Earth and Planetary Science Letters, 2021, 567, 117013.	4.4	5
77	Reply to the comment on "Chronostratigraphy and paleoclimatology of the LodÃ`ve Basin, France: Evidence for a pan-tropical aridification event across the Carboniferous–Permian boundary―by Michel et al., (2015). Palaeogeography, Palaeoclimatology, Palaeoecology 430, 118–131. Palaeogeography, Palaeoclimatology. Palaeoecology. 2016. 441. 1000-1004.	2.3	4
78	A Laurentian cratonic reference from the distal Proterozoic basement of Western Newfoundland using tandem <i>in situ</i> and isotope dilution U-pb zircon and titanite geochronology. Numerische Mathematik, 2021, 321, 1045-1079.	1.4	4
79	Synchronous emplacement of the anorthosite xenolithâ€bearing Beaver River diabase and one of the largest lava flows on Earth. Geochemistry, Geophysics, Geosystems, 2021, 22, e2021GC009909.	2.5	3
80	U-Pb geochronology and cyclostratigraphy of the middle Ediacaran upper Jibalah Group, eastern Arabian Shield. Precambrian Research, 2022, 375, 106674.	2.7	1